

1 **Intracellular replication of *Streptococcus pneumoniae* inside splenic macrophages serves**  
2 **as a reservoir for septicaemia**

3

4

5 Giuseppe Ercoli<sup>1</sup>, Vitor E. Fernandes<sup>2</sup>, Wen Y. Chung<sup>3</sup>, Joseph J Wanford<sup>1</sup>, Sarah Thomson<sup>4</sup>,  
6 Christopher D. Bayliss<sup>1</sup>, Kornelis Straatman<sup>5</sup>, Paul R. Crocker<sup>4</sup>, Ashley Dennison<sup>3</sup>, Luisa  
7 Martinez-Pomares<sup>6</sup>, Peter W. Andrew<sup>2</sup>, E. Richard Moxon<sup>7</sup>, Marco R. Oggioni<sup>1,\*</sup>

8

9

10 <sup>1</sup> Department of Genetics, University of Leicester, UK

11 <sup>2</sup> Department of Infection Immunity and Inflammation, University of Leicester, UK

12 <sup>3</sup> Hepato-Pancreato-Biliary (HPB) Unit, Leicester General Hospital, University of Hospitals of  
13 Leicester, NHS Trust, UK

14 <sup>4</sup> Division of Cell Signalling and Immunology, School of Life Sciences, University of Dundee, UK

15 <sup>5</sup> Centre for Core Biotechnology Services, University of Leicester, UK

16 <sup>6</sup> School of Life Sciences, Faculty of Medicine & Health Sciences, University of Nottingham, UK

17 <sup>7</sup> Department of Pediatrics, University of Oxford, UK

18

19

20

21

22

23

24 \* Address correspondence to Marco R. Oggioni, to Department of Genetics, University of  
25 Leicester, LE1 7RH Leicester , UK; email [mro5@leicester.ac.uk](mailto:mro5@leicester.ac.uk); phone +44 116 2252261

26

27

28

29 Word count: abstract 191, manuscript 3980

30 Character count: title 119 (suggested by the editor)

31

32

33 **INTRODUCTORY PARAGRAPH**

34

35 Bacterial septicaemia is a major cause of mortality, but its pathogenesis remains poorly  
36 understood. In experimental pneumococcal murine intravenous infection, an initial reduction  
37 of bacteria in the blood is followed hours later by a fatal septicaemia. These events  
38 represent a population-bottleneck driven by efficient clearance of pneumococci by splenic  
39 macrophages and neutrophils, but as we show here, accompanied by occasional  
40 intracellular replication of bacteria that are taken up by a sub-set of CD169-positive splenic  
41 macrophages. In this model, proliferation of these sequestered bacteria provides a reservoir  
42 for dissemination of pneumococci into the bloodstream, as demonstrated by its prevention  
43 using an anti-CD169 mAb treatment. Intracellular replication of pneumococci within CD169+  
44 splenic macrophages was also observed in an *ex vivo* porcine spleen, where the  
45 microanatomy is comparable to humans. We also showed that macrolides, that effectively  
46 penetrate macrophages, prevented septicaemia whereas beta-lactams, with inefficient  
47 intracellular penetration, failed to prevent dissemination to the blood. Our findings define a  
48 shift in our understanding of the pneumococcus from an exclusively extracellular pathogen to  
49 one with an intracellular phase. These findings open the door to the development of  
50 treatments that target this early, previously unrecognized intracellular phase of bacterial  
51 sepsis.

52

53

## 54 INTRODUCTION

55  
56 Despite the existence of highly evolved mechanisms of immunity, humans may still develop life-  
57 threatening sepsis<sup>1</sup>. Clinical management of sepsis is challenging and the discouraging outcome  
58 of many anti-sepsis trials plus increasing incidence of antimicrobial resistance are among the  
59 compelling reasons for further research to better understand the pathogenesis of invasive  
60 infection (septicaemia) and sepsis<sup>2</sup>. The bacterium *Streptococcus pneumoniae* (pneumococcus)  
61 is one of the major causes of serious disease and death<sup>3</sup>. About half of patients with  
62 pneumococcal pneumonia are septicaemic and the presence of bacteria in the blood correlates to  
63 disease severity and outcome<sup>4</sup> but it is not known why only a proportion of patients are  
64 septicaemic when there are no obvious co-morbidities or risk factors<sup>5</sup>. Notwithstanding decades  
65 of clinical and experimental research, there remain major gaps in our understanding of the early  
66 events in invasive pneumococcal infection<sup>6</sup>. Major unanswered questions are how pneumococci  
67 sustain a septicaemia that develops into clinical sepsis. Following intravenous inoculation of  
68 pneumococci in animals there is a consistent infection pattern in which a rapid reduction in the  
69 numbers of bacteria occurs such that within hours few, if any, organisms are detectable in the  
70 blood, a stage known as the 'eclipse phase'<sup>7,8</sup>. In animals lacking adaptive immunity to the  
71 pneumococcus, this eclipse phase results from innate immune clearance of bacteria by splenic  
72 macrophages but, depending on the virulence of the pneumococcal strain, it may later be  
73 followed by the emergence of septicaemia and lethal sepsis<sup>9</sup>. Recently, time-lapse microscopy  
74 observations have added important data on the dynamic role of neutrophils in the containment of  
75 pneumococcal infection a few hours after infection<sup>10</sup>. However, the host and microbial  
76 determinants of the transition from the contained infection during the eclipse phase to overt  
77 septicaemia and sepsis remain poorly understood.

78  
79 Previously we showed that the eclipse involves a single-cell population bottleneck<sup>8,11</sup>, which is  
80 succeeded by a 'recovery phase' with detection in the blood of pneumococci derived in most  
81 cases from clonal expansion of one founder bacterium. These events raised the critical question  
82 of how, within a few hours of virtual elimination of bacteria from the blood, a single founding  
83 pneumococcus could result in septicaemia. We hypothesised an extravascular site of  
84 pneumococcal replication, most likely in the spleen, because it is the major site of pneumococcal  
85 clearance<sup>12-14</sup>. Accordingly, we investigated the temporal pattern of localisation of bacteria in the  
86 spleen following intravenous inoculation. In particular, we investigated the involvement of different  
87 splenic macrophages. Here we show that the splenic metallophilic macrophages that are both  
88 CD169+ (Siglec-1, Sialoadhesin) and sulphated glycan positive (mannose receptor binding  
89 glycans; MRG+) <sup>15,16</sup>, henceforth referred to as CD169+act as a "sanctuary" during the first hours  
90 of pneumococcal infection. Our data reveal that septicaemia is initiated following uptake of

91 pneumococci by CD169+ macrophages in mice and pigs. Within the CD169+ macrophages the  
92 internalised bacteria evade clearance, undergo replication, then cause macrophage lysis and  
93 disseminate to the blood. Further, we show that antimicrobial therapy, specifically targeted to  
94 abort this phase of intracellular replication, can prevent the occurrence of pneumococcal  
95 septicaemia.

96

97

98

## 99 **RESULTS**

100

### 101 **Live pneumococci are present in the spleen prior to septicaemia.**

102 To investigate the events leading to the eclipse phase and the subsequent occurrence of  
103 septicaemia, we hypothesised that there was an extravascular reservoir of pneumococci in the  
104 spleen. We induced pneumococcal infection in mice by intravenous inoculation of  $1 \times 10^6$   
105 pneumococci. Consistent with previous results<sup>8</sup>, bacteria were still present in the blood at 6 hours  
106 (h) after challenge, but were effectively cleared at 8h (eclipse phase). Following the virtual  
107 elimination of bacteria from the blood, bacteria re-appeared following the eclipse phase and by  
108 24h mice showed signs of systemic infection (Fig. 1a). Using confocal microscopy, bacteria were  
109 visualised within the spleen during the eclipse phase (6 and 8h). Several staining combinations  
110 on tissue sections have been used to see the different splenic compartments (Supplementary  
111 Figure 1 a-b-c), showing the bacteria localised mainly in the marginal zone, the area surrounding  
112 the white pulp (Fig. 1c-d; Supplementary Figure 1 f-g). Higher magnification, revealed that  
113 bacteria were present as discrete clusters within the splenic tissue (Fig. 1e). In contrast, we did  
114 not detect bacteria in cultures of lung, cervical lymph node, liver and kidney homogenates at 8h.

115

### 116 **Foci of infection are founded by a single bacterium**

117 To further characterise the details of the persistence of pneumococci in the spleen, mice were  
118 sacrificed at 5 minutes (min), 30 min, 4 h, 6h and at 8h post-challenge with  $1 \times 10^6$  pneumococci.  
119 Five and thirty min post-challenge, microscopy of spleen sections demonstrated only single  
120 bacterial cells or diplococci, localised mainly to the marginal zone macrophages in the marginal  
121 sinus (Fig. 2a; Supplementary figure 1 d). In contrast, at 4, 6 and 8h after challenge,  
122 pneumococci were predominantly in the marginal zone metallophilic macrophages (Fig. 1c-d; Fig.  
123 2 b-d, Supplementary figure 1 e-g). The number of pneumococci in the clusters within the  
124 metallophilic macrophages increased over time (Fig. 2b-e). At 8h bacterial clusters appeared to  
125 extend to several adjacent host cells (Fig. 2d) and there were some single bacteria foci (Fig. 2e).  
126 These observations suggested lysis of infected cells, and release of bacteria to establish newly  
127 infected host cells.

128 To determine if the clusters of pneumococci originated as the result of the replication of single  
129 pneumococci, or through sequential phagocytic events by host cells, mice were inoculated  
130 intravenously with a 1:1 mixture of D39 strains expressing green fluorescent protein (GFP) or red  
131 fluorescent protein (RFP)<sup>17</sup>. The results showed that bacterial foci at 6h post-challenge consisted  
132 entirely of either green or red fluorescent bacteria (Fig. 2f). Multiple spleen samples showed  
133 complete absence of dual-labelled foci (2 spleens, 30 fields, Supplementary Table 2), clearly  
134 demonstrating that each infection focus was initiated by a single founder bacterium. Based on  
135 this finding and the bacterial counts within a focus (Fig. 2a-e), we estimated a mean generation  
136 time of approximately 60 min for pneumococcal replication within splenic tissue macrophages (5  
137 generations of 60 min from 1 cell after 1h of infection to 32 cells at 8h). Comparable foci of  
138 infection were detected when mice were infected with a serotype 4 strain TIGR4 or a non-  
139 capsulated derivative of D39 (Supplementary Figure 2).

140 Previous work demonstrated the detrimental effect of neutrophil (PMN) depletion on bacterial  
141 clearance during the eclipse phase<sup>8</sup>. Therefore, we investigated the presence of neutrophils in  
142 spleen sections at 0, 6 and 8h post-challenge. Consistent with the recent observation showing  
143 involvement of mobile PMNs in early splenic clearance of pneumococci<sup>10</sup>, we detected PMNs at  
144 all times almost exclusively in the red pulp (Fig. 2 g) with an increase in number over time (Fig. 2  
145 k). This increase was not uniform; PMNs localised next to pneumococcal cells and the number of  
146 PMNs per bacterial cluster also increased when comparing the samples at 6 and 8h (Fig. 2l).  
147 Clusters of pneumococci in red pulp macrophages were surrounded by PMNs (Fig. 2h), but  
148 neutrophils were not seen during the first 8 h in the proximity of the infectious foci in the marginal  
149 zone macrophages (Fig. 2i) or metallophilic macrophages (Fig. 2j).

150

### 151 **CD169+ macrophages preferentially accumulate pneumococci**

152 Soon after challenge, most bacteria were found next to the marginal sinus, the region where  
153 macrophages sample foreign antigens<sup>18</sup>. To investigate the fate of bacteria within the spleen, the  
154 distribution and number of infectious foci was determined 6h after intravenous challenge with 10<sup>6</sup>  
155 CFU/animal (Fig. 3 a). The compartments considered for this analysis were the white pulp,  
156 containing B and T cells (B220+ and KT3+ respectively), the marginal metallophilic macrophage  
157 area (CD169+ and MRG+)<sup>15,16</sup>, the marginal zone macrophage area (SIGN-R1+) and the red pulp  
158 (F4/80+) (Supplementary Figure 3 a-c). At this dose, the majority of infectious foci were in the red  
159 pulp (Supplementary Figure 3). After infection with a lower dose (10<sup>5</sup> CFU/animal) the clusters of  
160 pneumococci were predominantly observed next to the marginal sinus, the location of the  
161 marginal zone macrophages and the metallophilic macrophages, on the outside and inside of the  
162 sinus respectively (Supplementary Figure 3). Since the size of each compartment differs, multiple  
163 images of whole spleen sections were acquired and analysed to normalise the counts in the  
164 different areas of the spleen (Supplementary Figure 4). After normalisation, the data clearly

165 showed that the proportion of infected CD169+ metallophilic macrophages, was significantly  
166 higher both at the high and at the low dose compared to any other compartment (Fig. 3a).  
167 Counting the number of bacteria present in the macrophage-associated clusters at 6h, showed  
168 marginal zone macrophages (MZM) harbouring mainly single bacteria, metallophilic  
169 macrophages (CD169+) with foci of about 4 bacteria and red pulp macrophages (F4/80+) with  
170 about 8 bacteria/focus (Fig. 3b).

171 The surface marker CD169, defining the metallophilic macrophages, previously was shown to be  
172 involved in the phagocytosis of sialylated bacteria<sup>19-21</sup>. While pneumococci are not sialylated, they  
173 possess sialidases, including NanA, that contains a sialic acid binding domain previously shown  
174 to be involved in adhesion and invasion of host cells<sup>22</sup>. To test if the surface protein NanA could  
175 be involved in macrophage uptake, we repeated the infection experiment with a *nanA* deletion  
176 mutant, that has reduced virulence (Fig. 3c), and two recombinant strains expressing either only  
177 the N-terminal lectin binding domain (NanAΔ290-786) or the C-terminal sialidase domain  
178 (NanAΔ76-282). Both the *nanA* deletion mutant and the lectin domain mutant, known to be  
179 involved in sialic-acid-mediated host cell binding and invasion<sup>22</sup>, showed reduction of the number  
180 of foci in the metallophilic macrophages (Fig. 3d). It should be noted that the *nanA*-recombinants  
181 are constructed on the background of the *nanA* deletion mutant and that the recombinant  
182 expressing the lectin-like domain (NanAΔ290-786) regains the capacity to localise to CD169+  
183 cells.

184

### 185 **CD169 macrophages are the source of bacteria causing invasive disease**

186 Guided by reports showing that anti-CD169 antibodies prevented uptake of porcine reproductive  
187 and respiratory virus (PRRSV) by CD169+ macrophages<sup>23</sup>, we treated mice intravenously with an  
188 anti-CD169 mAb (Rat IgG2a,k, Clone: 3D6.112) 30 minutes prior to i.v. challenge with bacteria.  
189 At 4h post-infection, treatment with anti-CD169 prevented formation of foci in the metallophilic  
190 macrophages (Fig 3f). At 24h post-infection, the treatment with anti-CD169 prevented  
191 bacteraemia in almost all mice (Fig.3g) and this correlated with increased survival at 72h (Fig 3h).  
192 At 72h post-infection (or at the disease severity endpoint) almost all the mice treated with the  
193 CD169 mAb did not have detectable bacteria in blood and spleen (Supplementary Figure 5 a). It  
194 should be noted that the CD169 mAb, used as a single dose prior to challenge, was still  
195 detectable on the metallophilic macrophage surface at the conclusion of the experiment  
196 (Supplementary Figure 5 d).

197 Having established the importance of CD169+ macrophages in the pathogenesis of  
198 pneumococcal sepsis in our i.v. murine challenge model, we next sought to investigate the  
199 specific role of the CD169 surface expression marker in the interaction between bacteria and  
200 metallophilic macrophages. We compared infections of CD169 knock out mice and isogenic  
201 C57/BL6 controls<sup>16</sup>. We found no difference in the bacterial counts in blood or spleen, nor in the

202 size of infectious foci in the spleen (Supplementary Figure 5 f-g-h-i). These findings provided no  
203 evidence to support a direct role of CD169 itself in mediating interactions between pneumococci  
204 and metallophilic macrophages. However, C57/BL6 mice differ from CD1 mice in that splenic  
205 clearance is less efficient, blood counts are 100 fold higher and there is no eclipse phase (Fig 1a-  
206 b and Supplementary Figure 5 f-g), which limits the validity of the data by not allowing to evaluate  
207 the role of metallophilic macrophages in pneumococcal sepsis founded by a single cell  
208 bottleneck.

209

### 210 **Intracellular localisation of pneumococci**

211 To investigate whether bacteria in a splenic focus were extracellular or intracellular we used a  
212 number of different approaches. To delineate host cell plasma membrane, splenic sections  
213 infected with GFP-expressing bacteria were labelled with WGA (wheat germ agglutinin). The  
214 infection foci at 4h post-infection were enclosed in single host cells. The use of GFP-expressing  
215 bacteria allowed differentiation of intact pneumococcal cells from lysed bacteria, as shown in the  
216 orthogonal view of a representative multi-stack image acquired using confocal microscopy (Fig.  
217 4a-c). This image showed a cluster of pneumococci clearly identifiable between the cell nucleus  
218 (DAPI+) and the plasma membrane (WGA+). Its localisation was confirmed after deconvolution  
219 and 3D reconstruction of the tissue (Fig. 4d-e). Additionally, transmission electron microscopy  
220 showed groups of bacteria that localised within the host cell cytoplasm, without evident  
221 delimitation by a vacuolar membrane (Fig. 4f-g). The fine characterisation of the subcellular  
222 localisation of the bacteria within cells was impossible with these whole organ sections and must  
223 await the establishment of a validated model of primary cell culture of splenic CD169+ tissue  
224 macrophages.

225 To provide further evidence of the intracellular location of pneumococci, we employed the  
226 excellent penetration of macrolide antibiotics into macrophages (10-40 mg/L cell:  
227 extracellular concentration ratio, C/E ratio), compared to beta-lactams (C/E ratio <0.2 mg/L)<sup>24</sup>. We  
228 hypothesised that we would detect differences in prevention of septicaemia in mice treated using  
229 an ultra-short course of each drug. Erythromycin (1.5 mg/animal; half-life 48 min; Minimum  
230 Inhibitory Concentration (MIC) 0.06 mg/L) and ampicillin (0.5 mg/animal, half-life 50 min, MIC  
231 0.12 mg/L) were administered intraperitoneally at 1 and 5h post-infection. The doses were  
232 calculated so that the plasma concentration of both drugs would decrease below the MIC by 11h  
233 post-infection. Both antibiotics were effective in clearing pneumococci from the blood in the first  
234 24h (Fig. 4h), but only erythromycin prevented later outgrowth of bacteria resulting in complete  
235 resolution of the infection and survival of mice (Fig. 4i-j). The ampicillin-treated animals showed a  
236 survival rate comparable to the control group treated with PBS (Fig. 4i). These data are in  
237 accordance with macrolides being effective in the sterilisation of an intracellular bacterial  
238 reservoir and thus prevention of late onset septicaemia.

239  
240  
241  
242  
243  
244  
245  
246  
247  
248  
249  
250  
251  
252  
253  
254  
255  
256  
257  
258  
259  
260  
261  
262  
263  
264  
265  
266  
267  
268  
269  
270  
271

### **A pig model confirming CD169+ replication-permissive splenic macrophages**

There are anatomical differences between human and mouse spleens. In particular, the human spleen has a relatively smaller white pulp, no marginal zone and importantly, the CD169+ macrophages localise to the perifollicular area, mostly associated to sheathed capillaries<sup>25,26</sup>. Human capillary sheaths are thus predicted to have a function similar to the marginal zone in mice and rats<sup>26</sup>. For these reasons, the use of a second model was of crucial importance to determine the potential for translation of our results to humans<sup>26</sup>. The porcine spleen represents a suitable model as it closely resembles its human counterpart, with a comparable microanatomy and subpopulations of splenic macrophages<sup>27,28</sup> where CD169 is expressed by the perifollicular sheath macrophages<sup>29,30</sup>. Importantly the porcine experimental pneumococcal infection model also shows an eclipse phase following challenge<sup>31</sup>. Based on previous experience with porcine organ perfusion models<sup>32</sup>, we set up a normothermic, *ex vivo* porcine spleen perfusion model to test the dynamics of pneumococcal infection. The model involves immediate perfusion of abattoir-sourced porcine spleens, followed by 5h perfusion with heparinised autologous blood. In this model it was possible to run a pneumococcal infection for 5h; long enough to study the critical early stages of infection. Thirty minutes after starting perfusion, the arterial circuit was injected with  $6.5 \times 10^7$  CFU *S. pneumoniae* D39 (almost  $10^5$  CFU/ml). Subsequently, blood samples, spleen biopsies, and blood-gas parameters were taken at 30 min, 2, 4 and 5h. While pneumococci grew with a normal doubling time in heparinised pig blood (Fig 5a), the counts in the blood samples of the *ex vivo* model showed a steady decrease over time, while counts in the spleen steadily increased (Fig. 5b). This indicated that the spleen was performing its clearance role in this infection model. This porcine perfusion model of infection mirrored the data obtained in the mouse model. Bacterial clusters were found in increased numbers over time (Fig. 5c-e). In addition, independent foci derived from single bacterial cells were observed after infection with a mixed population of GFP- and RFP-expressing pneumococci (Fig. 5f-h). CD169+ macrophages in the porcine spleen localised in the peri-follicular zone (Fig. 5i-j). Analysis of spleen biopsies showed that, 5h post-infection, all foci of pneumococci were in CD169+ macrophages. The data from this whole organ pig model confirmed that early after infection single pneumococci are taken up by CD169+ macrophages and that these cells are permissive for rapid bacterial replication.



272

273 **DISCUSSION**

274

275 A conspicuous deficiency in our understanding of the pathophysiology of sepsis has been in  
276 detailing the host-microbial interactions occurring before the triggering of the catastrophic host  
277 inflammatory responses that are characteristic of overwhelming sepsis. Even when initially  
278 infected with many thousands of bacteria, our previous research showed that pneumococcal  
279 septicaemia is initiated by a single bacterial cell<sup>8,33</sup>. Recent data have reported the dynamics of *S.*  
280 *pneumoniae* clearance dependent on red pulp and marginal zone macrophages, aided by mobile  
281 neutrophils<sup>10</sup>. However, neither our work on the single cell bottleneck<sup>8,33</sup>, nor the time-lapse  
282 imaging of pneumococcal clearance in the spleen<sup>10</sup>, provided knowledge of how the founding  
283 organisms survive the highly efficient host innate immunity mechanisms. Now, here we have  
284 shown that a small number of bacteria occur within CD169-positive macrophages within the  
285 spleen and that these host cells represents an immune-privileged sanctuary and a reservoir for  
286 the reseeded of bacteria into the blood to cause septicaemia and sepsis. Importantly, these  
287 findings are not exclusively based on the murine model, but are confirmed by data in the pig; a  
288 model of high functional relevance and predictive value for humans<sup>27,28</sup>. There is an obvious  
289 difference between the mouse and pig i.v. challenge models, which are designed to study events  
290 in sepsis in the absence of pneumonia, and the most frequent human invasive disease which is  
291 sepsis associated with pneumonia. Thus, other studies are required, including human clinical or  
292 autopsy samples, to establish the relative importance of the spleen, and intracellular replication  
293 therein, in the development of sepsis in the presence and absence of overt pneumonia. In  
294 addition to giving a revised perspective on early events leading to septicaemia, our observations  
295 have immediate therapeutic implications because they show that septicaemia and sepsis can be  
296 prevented by early short term administration of antimicrobials that target the early intracellular  
297 bacterial population. In the demonstration of this conclusion, macrolides were much superior to  
298 beta-lactams, presently the first choice therapy for pneumococcal pneumonia<sup>5</sup>, in preventing  
299 septicaemia. This is perfectly in line with the call for intracellularly active drugs to fight multi-drug  
300 resistant staphylococcal infections, another extracellular pathogens found to hide in intracellular  
301 sanctuaries<sup>34</sup>.

302

303 In a murine model of pneumococcal sepsis, we have documented the importance of replication  
304 within splenic CD169+ metallophilic macrophages, as an anti-CD169 antibody blocked bacterial  
305 uptake into these cells and protected against subsequent invasive disease. CD169 (Siglec-1 or  
306 Sialoadhesin) is a surface lectin receptor of macrophages reported to be involved in binding and  
307 uptake of a variety of sialylated viruses and bacteria<sup>19-21,35,36</sup> but a role of CD169 in uptake of non-  
308 sialylated bacteria, such as pneumococci, has not been previously reported. It does appear,

309 however, that sialic acid recognition by pneumococci is important because a mutant bacteria  
310 lacking the main pneumococcal sialidase, NanA, or the lectin domain of NanA showed reduced  
311 localisation to the metallophilic macrophages. Significantly, the lectin domain of NanA has  
312 previously shown to be required for sialic acid mediated invasion in other tissues <sup>22</sup>, consistent  
313 with the suggestion that NanA mediates binding of pneumococci to macrophages, most likely to  
314 sialylated surface proteins. We conclude that while CD169 positive cells are critical, CD169 itself  
315 might not be directly involved.

316 To further examine the role of CD169 we infected CD169 KO mice, which still show the same  
317 ringlike distribution of MGR+ metallophilic macrophages around the white pulp (Fig. 5Si). As we  
318 saw that pneumococci localised to the marginal metallophilic macrophages with equal abundance  
319 in the knock out mice and the wt controls, this implies that CD169 is not directly involved in  
320 pneumococcal uptake into these macrophages and that the anti-CD169 antibodies are preventing  
321 infection of marginal metallophilic macrophages through indirect effects. For example, if CD169  
322 exists in a molecular complex with other molecule(s) required for pneumococcal uptake by  
323 macrophages, antibodies directed to CD169 could block their function through steric effects. It  
324 has also been demonstrated that under some circumstances antibodies to CD169 can trigger  
325 endocytosis and non-specifically affect phagocytosis of latex beads and bacteria<sup>37</sup>. Nevertheless,  
326 the message of the studies reported here is that pneumococcal interaction with CD169+  
327 macrophages in the spleen can be a critical precursor of septicaemia and sepsis. Invasive  
328 pneumococcal disease defined as bacteraemia without known primary focus or humans .

329  
330 The functions of CD169+ macrophages are poorly defined but there are no reports that they  
331 represent a classical anti-microbial cell populations. Indeed pneumococcal survival and growth  
332 has not been reported in “typical” macrophages<sup>8,38-41</sup>, including splenic red pulp macrophages<sup>10</sup>.  
333 To date, CD169+ metallophilic macrophages have been implicated mainly in induction of  
334 adaptive immunity by enhancing antigen availability for CD8 T cell and B cell activation, as shown  
335 by their permissiveness for viral replication in mice and pigs<sup>42,43</sup>. Adaptations enabling productive  
336 viral infection in CD169+ cells include upregulation of Usp18, which inhibits signalling through the  
337 IFN- $\alpha$  and IFN- $\beta$  receptors. CD169+ macrophages also have been shown to express higher  
338 levels of suppressors of cytokine signalling, which suggests unresponsiveness of these cells to  
339 selected stimuli<sup>42,43</sup>. CD169+ macrophages migrate to B cell follicles after LPS stimulation and  
340 this correlates with enhanced antibody responses to antigens targeted to these cells indicating  
341 that these macrophages can sense inflammatory stimuli<sup>44,45</sup>. Our data now show that they have a  
342 broader permissive state to infection than previously understood and that this permissive state  
343 includes intracellular bacterial replication. Combining this finding with the lack of neutrophil  
344 recruitment to the vicinity of infected CD169+ macrophages suggests that CD169+ macrophages

345 are an Achilles heel of innate immunity to pneumococcal infections and this extracellular  
346 pathogen exploits their relatively ineffective bactericidal mechanisms.

347  
348 For some bacterial pathogens an intracellular phase is well-known, for example *Salmonella*  
349 spp.<sup>46</sup>, and events leading to its invasive infection have been defined. However comparable data,  
350 especially insight from translational models, is not available for many pathogens, including the  
351 pneumococcus, whose within-host life style has been considered as extracellular. The  
352 intracellular phase described here documents a significant departure from accepted dogma. It  
353 alters perceptions of how pneumococcal bacteraemia occurs, despite efficient clearance  
354 mechanisms provided in the spleen, jointly by macrophages, complement and neutrophils<sup>10</sup>. It is  
355 remarkable that, despite life-threatening septicaemia being a relatively commonplace  
356 occurrence, so many gaps in our knowledge exist, including the tissue origins of bacteria and  
357 how they enter the vascular compartment and what leads to their replication to cause  
358 septicaemia<sup>47</sup>. Nevertheless a major lesson from the historical literature is that the sustained  
359 presence of bacteria in the blood cannot be plausibly explained by the one-off entry into the  
360 blood, but likely requires an extravascular immune-privileged focus<sup>48,49</sup>, which once identified  
361 can alter strategies for intervention<sup>34</sup>. In the present studies, we identify such a crucial  
362 extravascular, intracellular site of replication in splenic macrophages that initiates dissemination  
363 of pneumococci. Importantly, the intracellular replication phase providing a jump start for single  
364 bacterial cells, also explains the generation of a monoclonal bacteraemia founded by a single-cell  
365 bottleneck that is observed at low multiplicities of infection<sup>8</sup>.

366  
367 In summary, our findings define a crucial intracellular phase in the pathogenesis of invasive  
368 disease caused by the pneumococcus, classically considered to be the quintessential example of  
369 an extracellular bacterial pathogen. While the relevance of our findings for subacute bacteraemia  
370 or bacteraemia without a known primary focus appears evident, the applicability of our findings  
371 for pneumonia-associated bacteraemia will have to be defined. The findings open the door to the  
372 investigation of treatments that target this early, previously unrecognised yet critical intracellular  
373 phase of bacterial sepsis. Judicious use of anti-host therapeutic strategies or antimicrobials  
374 capable of efficient penetration of host cells may abort this crucial phase that is essential for  
375 initiating bacterial dissemination<sup>50</sup>. At the early intracellular stage in the pathogenesis, the  
376 numbers of organisms that need to be destroyed are relatively small, because this coincides with  
377 an extreme population bottleneck. Eliminating small numbers of intracellular bacteria is less  
378 challenging than contending with a much larger biomass, or even biofilm, consisting of millions of  
379 extracellular bacteria typical of the later stages of sepsis.

380

381

382 **Methods**

383

384 Pneumococcal strains and growth conditions

385 *S. pneumoniae* strain D39 (serotype 2), its non-encapsulated derivative R6<sup>51,52</sup>, a  
386 sialidase/neuraminidase *nanA* (SPD\_RS07935) deletion mutant<sup>53</sup>, the serotype 4 strain TIGR4<sup>54</sup>,  
387 and GFP and RFP fluorescent D39 (kindly provided by Jan Willem Veening, Groningen)<sup>17</sup>, were  
388 used in this study. A capsule deletion mutant of D39 expressing GFP was constructed by  
389 replacing the capsule locus with a kanamycin cassette<sup>55</sup>. All pneumococcal strains were cultured  
390 in Tryptic Soy Broth (TSB, Becton Dickinson) which in the case of green fluorescent (GFP) and  
391 red fluorescent (RFP) D39 was supplemented with 5 mg/L chloramphenicol (Sigma-Aldrich).  
392 Strains were also grown on blood agar plates consisting of Tryptic Soy Agar (Becton Dickinson)  
393 supplemented with 3% v/v defibrinated horse blood. All strains were cultured at 37°C, 5% v/v  
394 CO<sub>2</sub>. For transformations, competence was induced by addition of competence stimulating  
395 peptide 1 (CSP-1) to a final concentration of 0.625 µg/mL.

396

397 Construction of *nanA* deletion mutants

398 Three *nanA* mutants were constructed in D39. One strain was constructed lacking the region  
399 encoding the sialidase domain (NanAΔ290-786), one lacking the lectin-like domain (NanAΔ290-  
400 786), and an inactivating insertion mutant. Unmarked mutants were constructed by transforming  
401 with PCR generated recombinant constructs (Supplementary Table 2) using a two step approach  
402 (Sung et al. 2001). Mutants showed absence of any SNP in the cloned portion by Sanger  
403 sequencing.

404

405 Ethics statement

406 All studies in Leicester utilising CD1 mice were performed in accordance with United Kingdom  
407 Home Office licence PPL60/4327 and P7B01C07A, and were approved by the University of  
408 Leicester Ethics Committee. All mice were scored for signs of disease<sup>56</sup>. Animals were culled at  
409 pre-determined time points, or at the point at which they showed moderate signs of disease in  
410 accordance with the Home Office Licence.

411 The animal protocols used for the KO mice in this study were approved by the Ethical Review  
412 Committee of the University of Dundee. All procedures were conducted according to the  
413 requirements of the United Kingdom Home Office Animals Scientific Procedures Act, 1986, under  
414 PPL PB232D3BA.

415

416 Mice

417 Eight-week old, female, outbred CD1 mice from Charles River (Margate, Kent CT9 4LT UK) were  
418 used in this study. Before use, mice were kept for at least 1 week under standard conditions, in

419 the Central Research Facility animal facility at the University of Leicester, according to its  
420 guidelines for the maintenance of laboratory animals<sup>57-60</sup>. Blood samples from mice were  
421 collected by cardiac puncture under terminal anaesthesia, and treated with 100 U/ml of heparin  
422 (Sigma Aldrich, UK) to prevent blood coagulation. Mice were culled by cervical dislocation and  
423 death confirmed before the organs (spleen, lung, kidneys, cervical lymph nodes and liver) were  
424 collected post mortem. Mouse organs were either homogenised in 1 ml of TSB containing 10%  
425 v/v glycerol, for quantification of colony forming units (CFU), or fixed and embedded for  
426 sectioning.

427 The generation of Sialoadhesin KO (CD169 KO) mice has previously been described<sup>16</sup>. All wild-  
428 type (WT) and CD169 KO mice used in experiments were derived from heterozygotes back-  
429 crossed for at least ten generations onto a C57BL/6J background. Animals were housed under  
430 specific pathogen-free conditions under standard housing conditions of 12h light cycle, 21°C and  
431 relative humidity of 55-65. Male WT and CD169 KO mice were used at 9-10 weeks for the  
432 confirmatory experiment and of 20 weeks for the pilot experiment.

433

#### 434 Infection experiments

435 A total of 132 CD1 mice were used in this study. Sample size calculations were based on long  
436 standing experience with the infection models used<sup>57-59</sup>. Mice were randomised to cages and  
437 were challenged intravenously (i.v.) as previously described<sup>57-59</sup> with  $1.1 \times 10^5$  or  $1 \times 10^6$   
438 CFU/mouse. At pre-set time points, pre-selected groups were sacrificed for the collection of blood  
439 and organ samples. Bacteria were enumerated by plating on selective medium. The bacterial  
440 doses for the experiments described herein were selected based on previous experience, in  
441 order to raise bacteraemia in at least 50% of the mice.

442 Experiments in C57BL/6J WT and CD169 KO mice included a confirmatory experiment using  
443  $n=6$ /group and a pilot experiment of  $n=3$ /group. Mice were infected with  $2 \times 10^6$  CFU/mouse with  
444 *S. pneumoniae* D39 via intravenous injection. Mice were monitored over a 6h period with no  
445 clinical signs observed. 6h post infection, mice were sacrificed by exposure to a rising  
446 concentration of carbon dioxide and blood taken by cardiac puncture. Whole blood was frozen in  
447 1 ml RPMI/15% glycerol. Spleen was removed and half stored in 1 ml RPMI/15% glycerol. The  
448 remaining half was embedded and frozen in OCT. All samples were processed in Leicester.

449 The operator carrying out the sample and data analysis was blinded for all experimnts regarding  
450 the C57BL/6J mice, but not for work on CD1 mice.

451

452

#### 453 CD169 blockade

454 Blockade experiments were performed by intravenously injecting 10 µg of anti-CD169 mAb (Rat  
455 IgG2a,k, Clone: 3D6.112), or isotype matched control (Rat IgG2a, clone RTK2758) 30 minutes

456 prior to intravenous infection with  $10^6$  CFU *S. pneumoniae* D39 through the lateral tail vein. The  
457 distribution of the anti-CD169 mAb was assessed in the spleen through microscopy of sections  
458 (Supplementary Figure 5 b). Blood was taken by tail bleed, 24 hours after infection, to enumerate  
459 the number of CFU in the blood. Mice were culled at 72 hours post-infection, or when they  
460 showed moderate signs of disease in accordance with the home office licence. Blood were taken  
461 by cardiac puncture at death, and spleens were either frozen in OCT, or homogenised, serially  
462 diluted and plated to count viable bacteria. In all cases, death was confirmed by cervical  
463 dislocation. Signs of disease were monitored throughout the course of the experiments. Two  
464 independent receptor blockade experiments were performed, each with two groups of 5 mice (20  
465 mice total).

466  
467 **Confocal Microscopy**  
468 Confocal imaging was performed on infected spleen sections and uninfected controls. The  
469 organs were frozen in dry ice, in Optimum Cutting Temperature (OCT) embedding matrix  
470 (Thermoscientific). A Leica CM1850UV cryostat was used to slice the tissues; 8  $\mu$ m thick sections  
471 were cut and mounted on gelatin coated microscopy slides. Organ sections were then dried for  
472 10 min at room temperature (RT) before fixing in phosphate-buffered saline (PBS) containing 4%  
473 v/v EM grade formaldehyde (Sigma) for 20 min at RT. Samples were washed three times in PBS,  
474 and incubated for 10 min with PBS containing 0.1% v/v Triton-x100 to permeabilise the tissues.  
475 Samples were then incubated for 30 min in blocking solution (PBS containing 5% v/v goat  
476 serum). Sections were incubated for 1 h with primary antibodies diluted in blocking solution,  
477 washed three times with PBS, and then incubated for 45 min with secondary antibody solution.  
478 Samples were then washed three times with PBS and once with H<sub>2</sub>O before adding the mounting  
479 medium containing DAPI (Thermoscientific ProLong Gold Antifade Mountant) and closing the  
480 slides with coverslips. Anti-serotype 2 and 4 capsule antibodies (Statens Serum Institute) were  
481 used to stain non-fluorescent bacteria. Different macrophages populations were labelled using a  
482 panel of antibodies (Supplementary Table 1). Metallophilic macrophages were labelled by anti-  
483 Mouse CD169 and the recombinant protein CR-Fc, which binds mannose receptor ligands  
484 expressed by the metallophilic CD169-positive macrophages<sup>61</sup>. Marginal zone macrophages  
485 were labelled with, anti-Mouse CD209b (SIGN-R1, eBioscience) and anti-Mouse F4/80 antibody  
486 (eBioscience). For other classes of immune cells, the following antibodies were used: anti-CD3  
487 (clone Kt3 specific for T cells), anti-B220 (specific for B cells) and anti-FDC-M1 mAb (4C11  
488 specific for follicular dendritic cells). For the studies of bacterial localisation Alexafluor 633-  
489 conjugated Wheat germ agglutinin and Alexafluor 647-conjugated phalloidin (Actin;  
490 Thermoscientific) were used. The porcine spleen samples were stained with anti-porcine CD169  
491 and anti-porcine CD163 (both Biorad) (Supplementary Table 1). Combinations of Alexafluor  
492 conjugated antibodies from Thermoscientific were used as secondary antibodies (488, 568 or 647

493 with different host specificity) (Supplementary Table 1). An Olympus FV1000 confocal laser  
494 scanning microscope was used to acquire the images using 20X and 60X objectives, and the free  
495 software ImageJ (<http://imagej.nih.gov/ij/>) was used for image processing. For visualization  
496 purpose some images were deconvolved using Huygens Essential deconvolution software  
497 version 16 (Scientific Volume Imaging, Netherlands) and viewed in Imaris 3D reconstruction  
498 software 9.4 (Bitplane, Switzerland).

499

#### 500 Scanning of microscopy sections and spleen area measurements

501 Spleen sections were stained with different combinations of antibodies in order to identify the  
502 different spleen compartments. The sections were scanned using a fully motorised Nikon Eclipse  
503 Ti microscope equipped with a Plan Fluor 10X/0.3 objective and an Andor iXonEM+ EMCCD DU  
504 885 camera. Automatic tissue scanning was performed using NIS-Elements software AR  
505 4.51 (Nikon, Japan) and the images obtained were analysed using ImageJ software 1.51. Using  
506 the DAPI signal, the total area of each tissue section was calculated. Four different spleen  
507 compartments were identified and their areas calculated: white pulp, metallophilic macrophages,  
508 marginal zone and red pulp macrophages. The white pulp areas were defined as those areas that  
509 stained with a combination of B220 (B cells), CD3 (T cells) enclosed within the metallophilic rings  
510 stained with Siglec-1 (metallophilic macrophages marker). The areas of metallophilic  
511 macrophages (Siglec-1), marginal zone macrophages (SIGN-R1) and red pulp macrophages  
512 (F4/80) were defined as those areas stained for each cell marker. The proportion of the spleen  
513 compartments with respect to the total was calculated using the data obtained from at least 5  
514 different images for each staining combination (Supplementary Figure 3). For neutrophils  
515 quantification cells were detected with an Ly-6G specific primary antibodies, and numbers of  
516 neutrophils were enumerated in at least 5 fields from 3 independent, biological replicates.

517

#### 518 Transmission Electron Microscopy

519 Excised tissue was primarily fixed with 4% v/v Formaldehyde / 0.5% Glutaraldehyde in sodium  
520 cacodylate buffer with 2uM of calcium chloride overnight, followed by several washes in same  
521 buffer. The samples were post-fixed with aqueous 1% w/v osmium tetroxide/ 1.5% w/v potassium  
522 ferrocyanide for 60 min, washed with distilled, de-ionised water, followed by a further 60 minutes  
523 in 1% w/v aqueous osmium. After further washes with DDW, the tissue was en bloc stained in 2%  
524 w/v aqueous uranyl acetate for 60 min. Following dehydration through an ethanol series, the  
525 samples were treated with several short washes through ice cold acetone, before gradual  
526 infiltration with Durcupan resin (Sigma-Aldrich UK). Once fully infiltrated with Durcupan, the tissue  
527 was embedded in BEEM capsules, and polymerised at 60°C for 48 h.

528 Thin sections, of approximately 80 nm thickness, were cut from each sample using a Leica UC7  
529 ultramicrotome, collected on copper mesh grids and counter stained Reynolds' lead citrate.

530 Sections were observed using a JEOL JEM-1400 transmission electron microscope, using an  
531 accelerating voltage of 100 kV. Digital Images were recorded using a SIS Megaview III Digital  
532 Camera (Olympus Soft Imaging Solutions, Germany) with ITEM Software V 5.1 (Olympus,  
533 Germany).

534

535 Porcine spleen perfusion model of infection

536 The methodology for perfusion of the porcine spleen was similar to that described previously for  
537 the perfusion of liver and kidney <sup>32</sup>. Porcine spleens were collected from a local abattoir from  
538 domestic Large White pigs (40–50kg) immediately after slaughter. Following a midline  
539 laparotomy, a splenectomy was carried out close to its hilum. To perfuse the organ, the celiac  
540 trunk was isolated and cannulated, while the other arteries were carefully ligated and divided. The  
541 spleen was then perfused with saline solution containing heparin (LEO Laboratories Limited, UK)  
542 and human urokinase (Syner-Medica Ltd, UK) through the main splenic artery, and the blood  
543 excess was flushed out through the main splenic vein. The perfusion set-up consists of a SARNS  
544 8000 extracorporeal roller pump (3M, St. Paul, MN, USA), Baby-RX venous reservoir and  
545 membrane oxygenator (Terumo, Ann Arbor, MI, USA), metal organ chamber, PVC tubings  
546 (Cellplex, Dandenong, VIC, Australia) and water bath temperature regulator.

547 The perfusate consisted of 1 litre of autologous whole blood collected via exsanguination,  
548 containing the two antimicrobials nalidixic acid (10 mg/L) and colistin (5 mg/L), glucose (5 ml/h),  
549 500 µg epoprostenol sodium (vasodilatation), and 5000 IU heparin (microclots prevention;  
550 1500units/hr). The temperature of the water bath was set at 39°C and oxygenation at 2 L/min.  
551 When the blood was warm and oxygenated, the organ was connected to the system. Initial flow  
552 rate was set at 0.2 L/min, adjusted to maintain a mean arterial pressure (MAP) at 70–80 mm Hg.  
553 As soon as the perfused spleen reached a stable flow (typically 30 min), the arterial circuit was  
554 injected with *S. pneumoniae*. Over the subsequent 5 h, serial blood samples and spleen biopsies  
555 were taken. Blood gas analysis was performed before and after the infection at predetermined  
556 time points to verify the functionality of the organ. Overall four infection perfusion experiments,  
557 and three negative controls using non-infected perfused organs were performed.

558

559 Statistical analysis

560 GraphPad Prism software version 6 was used to analyse all data. Fisher's exact test was used to  
561 compare different cohorts of mice with the assumption that all samples containing more than 100  
562 CFU/ml (or CFU/mg) were positive and the others negative. One-way Anova, with Tukey's post-  
563 test, was used to compare the distribution of foci of bacteria in the spleen. Survival curves have  
564 been compared with a Log-rank (Mantel-Cox) test. Results were considered significant when P  
565 values were <0.05. Error bars in all figures show the Standard Deviation, unless otherwise stated.

566



567 Data availability

568 The data that support the findings of this study are available from the corresponding author upon  
569 request. The recombinant protein CR-Fc, which binds mannose receptor ligands expressed by  
570 the metallophilic CD169-positive macrophages can be obtained for Luisa Martinez-Pomares and  
571 the CD169 knock out mice and their isogenic C57/BL6 controls can be obtained from Paul  
572 Crocker.

573

574 **Statement on Data and Materials request**

575 For any correspondence regarding data and results please contact Marco R Oggioni  
576 (mro5@leicester.ac.uk), for access to the recombinant protein CR-Fc please contact Luisa  
577 Martinez-Pomares (luisa.m@nottingham.ac.uk) and for access to the CD169 knock out mice and  
578 their isogenic C57/BL6 controls please contact Paul Crocker (p.r.crocker@dundee.ac.uk).

579

580

581 **Acknowledgements**

582 GE was funded through an academic collaboration agreement between the Universities of Oxford  
583 and Leicester and in part by MRC grant MR/M003078/1. Authors would like to thank Jan Willem  
584 Veening for providing GFP and RFP pneumococci, Francesca Focarelli for construction of the  
585 non-encapsulated GFP expressing strain, Megan De Ste Croix for mutant construction, Sarah  
586 Glenn for help with the infection experiments, the Electron Microscopy Facility, University of  
587 Leicester for their technical support and Rohan Kumar and John Isherwood for help with the  
588 perfusion of the porcine organs at explant, the staff of Joseph Morris Butchers Ltd, Michael F  
589 Wood Butchers and the staff of Leicester Preclinical Research Facility for support.

590

591

592 **Author contributions**

593 G.E. performed almost all experiments and wrote the manuscript. V.E.F. led and performed the  
594 animal infections. W.Y.C. led and performed the porcine spleen perfusion experiments. J.J.W.  
595 contributed to microscopy, animal infection work and contributed to the writing of the manuscript.  
596 C.D.B. contributed to the design of the experimental work. K.S. led the microscopy work. S.T.  
597 performed the infections of the CD169 ko mice. P.C. discussed the work and supervised the  
598 infections in the ko mice and contributed to the writing of the manuscript. A.D. designed and led  
599 the porcine perfusion work and contributed to the writing of the manuscript. L.M.P. designed the  
600 immunological work and overall setup of experimentation and contributed to the writing of the  
601 manuscript. P.W.A. participated in the overall design and setup of the experimentation and  
602 contributed to the writing of the manuscript. E.R.M. initiated and participated in the overall design  
603 and setup of the experimentation and contributed to the writing of the manuscript. M.R.O. led the  
604 design and setup of the project and contributed to the writing of the manuscript.

605

606

607 **Competing interests**

608 The authors declare no competing interests.

609

610

611 **References**

- 612
- 613 1 Gratz, N., Loh, L. N. & Tuomanen, E. in *Streptococcus Pneumoniae* (eds Sven  
614 Hammerschmidt & Carlos Orihuela) 433-451 (Academic Press, 2015).
- 615 2 van der Poll, T. Future of sepsis therapies. *Critical Care* **20**, 106,  
616 doi:10.1186/s13054-016-1274-9 (2016).
- 617 3 WHO. Pneumococcal vaccines WHO position paper. *WHO, Weekly Epidemiological*  
618 *Record (WER)* **87**, 129–144 (2012). <<http://www.who.int/wer/2012/wer8714/en/>>.
- 619 4 Musher , D. M. & Thorner , A. R. Community-Acquired Pneumonia. *New England*  
620 *Journal of Medicine* **371**, 1619-1628, doi:doi:10.1056/NEJMra1312885 (2014).
- 621 5 Lim, W. S., Smith, D. L., Wise, M. P. & Welham, S. A. British Thoracic Society  
622 community acquired pneumonia guideline and the NICE pneumonia guideline: how  
623 they fit together. *Thorax*, doi:10.1136/thoraxjnl-2015-206881 (2015).
- 624 6 Simell, B. *et al.* The fundamental link between pneumococcal carriage and disease.  
625 *Expert Review of Vaccines* **11**, 841-855, doi:10.1586/erv.12.53 (2012).
- 626 7 Rogers, D. E. HOST MECHANISMS WHICH ACT TO REMOVE BACTERIA FROM  
627 THE BLOOD STREAM. *Bacteriological Reviews* **24**, 50-66 (1960).
- 628 8 Gerlini, A. *et al.* The Role of Host and Microbial Factors in the Pathogenesis of  
629 Pneumococcal Bacteraemia Arising from a Single Bacterial Cell Bottleneck. *PLoS*  
630 *Pathogens* **10**, e1004026, doi:10.1371/journal.ppat.1004026 (2014).
- 631 9 Brown, E. J., Hosea, S. W. & Frank, M. M. The role of the spleen in experimental  
632 pneumococcal bacteremia. *Journal of Clinical Investigation* **67**, 975-982 (1981).
- 633 10 Deniset, J. F., Surewaard, B. G., Lee, W.-Y. & Kubes, P. Splenic  
634 Ly6G<sup>high</sup> mature and Ly6G<sup>int</sup> immature neutrophils  
635 contribute to eradication of *S. pneumoniae*. *The Journal of Experimental*  
636 *Medicine* **214**, 1333-1350, doi:10.1084/jem.20161621 (2017).
- 637 11 Kono, M. *et al.* Single Cell Bottlenecks in the Pathogenesis of Streptococcus  
638 pneumoniae. *PLoS Pathogens* **12**, e1005887, doi:10.1371/journal.ppat.1005887  
639 (2016).
- 640 12 Horan, M. & Colebatch, J. H. Relation Between Splenectomy and Subsequent  
641 Infection: A Clinical Study. *Archives of Disease in Childhood* **37**, 398-414 (1962).
- 642 13 Theilacker, C. *et al.* Overwhelming Postsplenectomy Infection: A Prospective  
643 Multicenter Cohort Study. *Clinical Infectious Diseases* **62**, 871-878,  
644 doi:10.1093/cid/civ1195 (2016).
- 645 14 Shinefield, H. R., Steinberg, C. R. & Kaye, D. EFFECT OF SPLENECTOMY ON THE  
646 SUSCEPTIBILITY OF MICE INOCULATED WITH DIPLOCOCCUS PNEUMONIAE.  
647 *The Journal of Experimental Medicine* **123**, 777-794 (1966).
- 648 15 Martinez-Pomares, L. *et al.* Fc chimeric protein containing the cysteine-rich domain  
649 of the murine mannose receptor binds to macrophages from splenic marginal zone  
650 and lymph node subcapsular sinus and to germinal centers. *The Journal of*  
651 *experimental medicine* **184**, 1927-1937 (1996).
- 652 16 Oetke, C., Vinson, M. C., Jones, C. & Crocker, P. R. Sialoadhesin-deficient mice  
653 exhibit subtle changes in B- and T-cell populations and reduced immunoglobulin M  
654 levels. *Molecular and cellular biology* **26**, 1549-1557, doi:10.1128/mcb.26.4.1549-  
655 1557.2006 (2006).
- 656 17 Kjos, M. *et al.* Bright Fluorescent Streptococcus pneumoniae for Live-Cell Imaging of  
657 Host-Pathogen Interactions. *Journal of Bacteriology* **197**, 807-818,  
658 doi:10.1128/JB.02221-14 (2015).
- 659 18 Aichele, P. *et al.* Macrophages of the Splenic Marginal Zone Are Essential for  
660 Trapping of Blood-Borne Particulate Antigen but Dispensable for Induction of Specific  
661 T Cell Responses. *The Journal of Immunology* **171**, 1148-1155,  
662 doi:10.4049/jimmunol.171.3.1148 (2003).
- 663 19 Jones, C., Virji, M. & Crocker, P. R. Recognition of sialylated meningococcal  
664 lipopolysaccharide by siglecs expressed on myeloid cells leads to enhanced bacterial

- 665 uptake. *Molecular Microbiology* **49**, 1213-1225, doi:10.1046/j.1365-  
666 2958.2003.03634.x (2003).
- 667 20 Heikema, A. P. *et al.* Enhanced, Sialoadhesin-Dependent Uptake of Guillain-Barré  
668 Syndrome-Associated *Campylobacter jejuni* Strains by Human Macrophages.  
669 *Infection and Immunity* **81**, 2095-2103, doi:10.1128/IAI.01437-12 (2013).
- 670 21 Chang, Y.-C. *et al.* Role of Macrophage Sialoadhesin in Host Defense Against the  
671 Sialylated Pathogen Group B *Streptococcus*. *Journal of molecular medicine (Berlin,*  
672 *Germany)* **92**, 951-959, doi:10.1007/s00109-014-1157-y (2014).
- 673 22 Uchiyama, S. *et al.* The surface-anchored NanA protein promotes pneumococcal  
674 brain endothelial cell invasion. *The Journal of Experimental Medicine* **206**, 1845-  
675 1852, doi:10.1084/jem.20090386 (2009).
- 676 23 Vanderheijden, N. *et al.* Involvement of sialoadhesin in entry of porcine reproductive  
677 and respiratory syndrome virus into porcine alveolar macrophages. *Journal of*  
678 *virology* **77**, 8207-8215 (2003).
- 679 24 Maurin, M. & Raoult, D. Antibiotic penetration within eukaryotic cells. *Antimicrobial*  
680 *Agents and Intracellular Pathogens*, 21-37 (1993).
- 681 25 Steiniger, B., Barth, P. & Hellinger, A. The Perifollicular and Marginal Zones of the  
682 Human Splenic White Pulp : Do Fibroblasts Guide Lymphocyte Immigration? *The*  
683 *American Journal of Pathology* **159**, 501-512 (2001).
- 684 26 Steiniger, B. S. Human spleen microanatomy: why mice do not suffice. *Immunology*  
685 **145**, 334-346, doi:10.1111/imm.12469 (2015).
- 686 27 Fairbairn, L., Kapetanovic, R., Sester, D. P. & Hume, D. A. The mononuclear  
687 phagocyte system of the pig as a model for understanding human innate immunity  
688 and disease. *Journal of Leukocyte Biology*, doi:10.1189/jlb.1110607 (2011).
- 689 28 Meurens, F., Summerfield, A., Nauwynck, H., Saif, L. & Gerdtts, V. The pig: a model  
690 for human infectious diseases. *Trends in Microbiology* **20**, 50-57,  
691 doi:<https://doi.org/10.1016/j.tim.2011.11.002> (2012).
- 692 29 Ezquerro, A. *et al.* Porcine myelomonocytic markers and cell populations.  
693 *Developmental & Comparative Immunology* **33**, 284-298,  
694 doi:<http://dx.doi.org/10.1016/j.dci.2008.06.002> (2009).
- 695 30 Alvarez, B. *et al.* Phenotypic and functional heterogeneity of CD169+ and CD163+  
696 macrophages from porcine lymph nodes and spleen. *Developmental & Comparative*  
697 *Immunology* **44**, 44-49, doi:<http://dx.doi.org/10.1016/j.dci.2013.11.010> (2014).
- 698 31 de Greeff, A. *et al.* Pneumococcal colonization and invasive disease studied in a  
699 porcine model. *BMC Microbiology* **16**, 102, doi:10.1186/s12866-016-0718-3 (2016).
- 700 32 Chung, W. Y. *et al.* Steps for the Autologous Ex vivo Perfused Porcine Liver-kidney  
701 Experiment. *Journal of Visualized Experiments : JoVE*, 50567, doi:10.3791/50567  
702 (2013).
- 703 33 Moxon, E. R. & Murphy, P. A. Haemophilus influenzae bacteremia and meningitis  
704 resulting from survival of a single organism. *Proceedings of the National Academy of*  
705 *Sciences of the United States of America* **75**, 1534-1536 (1978).
- 706 34 Lehar, S. M. *et al.* Novel antibody–antibiotic conjugate eliminates intracellular *S.*  
707 *aureus*. *Nature* **527**, 323-328, doi:10.1038/nature16057 (2015).
- 708 35 Heikema, A. P. *et al.* Characterization of the Specific Interaction between  
709 Sialoadhesin and Sialylated *Campylobacter jejuni* Lipooligosaccharides. *Infection*  
710 *and Immunity* **78**, 3237-3246, doi:10.1128/IAI.01273-09 (2010).
- 711 36 Klaas, M. *et al.* Sialoadhesin Promotes Rapid Proinflammatory and Type I IFN  
712 Responses to a Sialylated Pathogen, *Campylobacter jejuni*. *The Journal of*  
713 *Immunology Author Choice* **189**, 2414-2422, doi:10.4049/jimmunol.1200776 (2012).
- 714 37 De Schryver, M. *et al.* Monoclonal antibody binding to the macrophage-specific  
715 receptor sialoadhesin alters the phagocytic properties of human and mouse  
716 macrophages. *Cellular immunology* **312**, 51-60, doi:10.1016/j.cellimm.2016.11.009  
717 (2017).

- 718 38 Bewley, M. A. *et al.* Pneumolysin Activates Macrophage Lysosomal Membrane  
719 Permeabilization and Executes Apoptosis by Distinct Mechanisms without Membrane  
720 Pore Formation. *mBio* **5**, e01710-01714, doi:10.1128/mBio.01710-14 (2014).
- 721 39 Dockrell, D. H., Lee, M., Lynch, D. H. & Read, R. C. Immune-Mediated Phagocytosis  
722 and Killing of *Streptococcus pneumoniae* Are Associated with Direct and Bystander  
723 Macrophage Apoptosis. *The Journal of Infectious Diseases* **184**, 713-722,  
724 doi:10.1086/323084 (2001).
- 725 40 Gordon, S. B., Irving, G. R. B., Lawson, R. A., Lee, M. E. & Read, R. C. Intracellular  
726 Trafficking and Killing of *Streptococcus pneumoniae* by Human Alveolar  
727 Macrophages Are Influenced by Opsonins. *Infection and Immunity* **68**, 2286-2293  
728 (2000).
- 729 41 Davis, K. M., Nakamura, S. & Weiser, J. N. Nod2 sensing of lysozyme-digested  
730 peptidoglycan promotes macrophage recruitment and clearance of *S. pneumoniae*  
731 colonization in mice. *The Journal of Clinical Investigation* **121**, 3666-3676,  
732 doi:10.1172/JCI57761 (2011).
- 733 42 Honke, N. *et al.* Enforced viral replication activates adaptive immunity and is  
734 essential for the control of a cytopathic virus. *Nat Immunol* **13**, 51-57,  
735 doi:[http://www.nature.com/ni/journal/v13/n1/abs/ni.2169.html#supplementary-](http://www.nature.com/ni/journal/v13/n1/abs/ni.2169.html#supplementary-information)  
736 [information](http://www.nature.com/ni/journal/v13/n1/abs/ni.2169.html#supplementary-information) (2012).
- 737 43 Van Breedam, W., Verbeeck, M., Christiaens, I., Van Gorp, H. & Nauwynck, H. J.  
738 Porcine, murine and human sialoadhesin (Sn/Siglec-1/CD169): portals for porcine  
739 reproductive and respiratory syndrome virus entry into target cells. *Journal of*  
740 *General Virology* **94**, 1955-1960, doi:doi:10.1099/vir.0.053082-0 (2013).
- 741 44 Backer, R. *et al.* Effective collaboration between marginal metallophilic macrophages  
742 and CD8(+) dendritic cells in the generation of cytotoxic T cells. *Proceedings of the*  
743 *National Academy of Sciences of the United States of America* **107**, 216-221,  
744 doi:10.1073/pnas.0909541107 (2010).
- 745 45 Veninga, H. *et al.* Antigen targeting reveals splenic CD169(+) macrophages as  
746 promoters of germinal center B - cell responses. *European Journal of Immunology*  
747 **45**, 747-757, doi:10.1002/eji.201444983 (2015).
- 748 46 Mastroeni, P., Grant, A., Restif, O. & Maskell, D. A dynamic view of the spread and  
749 intracellular distribution of *Salmonella enterica*. *Nat Rev Micro* **7**, 73-80 (2009).
- 750 47 Levin, B. R. & Antia, R. Why We Don't Get Sick: The Within-Host Population  
751 Dynamics of Bacterial Infections. *Science* **292**, 1112-1115,  
752 doi:10.1126/science.1058879 (2001).
- 753 48 Shaw, S., Smith, A. L., Anderson, P. & Smith, D. H. The paradox of *Hemophilus*  
754 *influenzae* type B bacteremia in the presence of serum bactericidal activity. *Journal of*  
755 *Clinical Investigation* **58**, 1019-1029 (1976).
- 756 49 Grant, A. J. *et al.* Modelling within-Host Spatiotemporal Dynamics of Invasive  
757 Bacterial Disease. *PLoS Biology* **6**, e74, doi:10.1371/journal.pbio.0060074 (2008).
- 758 50 Surewaard, B. G. J. *et al.* Identification and treatment of the *Staphylococcus*  
759 *aureus* reservoir in vivo. *The Journal of Experimental Medicine*,  
760 doi:10.1084/jem.20160334 (2016).
- 761 51 Avery, O. T., MacLeod, C. M. & McCarty, M. STUDIES ON THE CHEMICAL  
762 NATURE OF THE SUBSTANCE INDUCING TRANSFORMATION OF  
763 PNEUMOCOCCAL TYPES : INDUCTION OF TRANSFORMATION BY A  
764 DESOXYRIBONUCLEIC ACID FRACTION ISOLATED FROM PNEUMOCOCCUS  
765 TYPE III. *The Journal of Experimental Medicine* **79**, 137-158 (1944).
- 766 52 Iannelli, F., Pearce, B. J. & Pozzi, G. The Type 2 Capsule Locus of *Streptococcus*  
767 *pneumoniae*. *Journal of Bacteriology* **181**, 2652-2654 (1999).
- 768 53 Manco, S. *et al.* Pneumococcal Neuraminidases A and B Both Have Essential Roles  
769 during Infection of the Respiratory Tract and Sepsis. *Infection and Immunity* **74**,  
770 4014-4020, doi:10.1128/IAI.01237-05 (2006).

771 54 Tettelin, H. *et al.* Complete Genome Sequence of a Virulent Isolate of  
772 *Streptococcus pneumoniae*. *Science* **293**, 498-506,  
773 doi:10.1126/science.1061217 (2001).

774 55 Pearce, B. J., Iannelli, F. & Pozzi, G. Construction of new unencapsulated (rough)  
775 strains of *Streptococcus pneumoniae*. *Research in Microbiology* **153**, 243-247,  
776 doi:[http://dx.doi.org/10.1016/S0923-2508\(02\)01312-8](http://dx.doi.org/10.1016/S0923-2508(02)01312-8) (2002).

777 56 Morton, D. & Griffiths, P. Guidelines on the recognition of pain, distress and  
778 discomfort in experimental animals and an hypothesis for assessment. *Veterinary*  
779 *Record* **116**, 431-436, doi:10.1136/vr.116.16.431 (1985).

780 57 Kadioglu, A. *et al.* Sex-Based Differences in Susceptibility to Respiratory and  
781 Systemic Pneumococcal Disease in Mice. *The Journal of Infectious Diseases* **204**,  
782 1971-1979, doi:10.1093/infdis/jir657 (2011).

783 58 Oggioni, M. R. *et al.* Antibacterial Activity of a Competence-Stimulating Peptide in  
784 Experimental Sepsis Caused by *Streptococcus pneumoniae*. *Antimicrobial Agents*  
785 *and Chemotherapy* **48**, 4725-4732, doi:10.1128/AAC.48.12.4725-4732.2004 (2004).

786 59 Oggioni, M. R. *et al.* Switch from planktonic to sessile life: a major event in  
787 pneumococcal pathogenesis. *Molecular Microbiology* **61**, 1196-1210,  
788 doi:10.1111/j.1365-2958.2006.05310.x (2006).

789 60 Lee, E.-J., Pontes, M. H. & Groisman, E. A. A Bacterial Virulence Protein Promotes  
790 Pathogenicity by Inhibiting the Bacterium's Own F(1)F(o) ATP Synthase. *Cell* **154**,  
791 146-156, doi:10.1016/j.cell.2013.06.004 (2013).

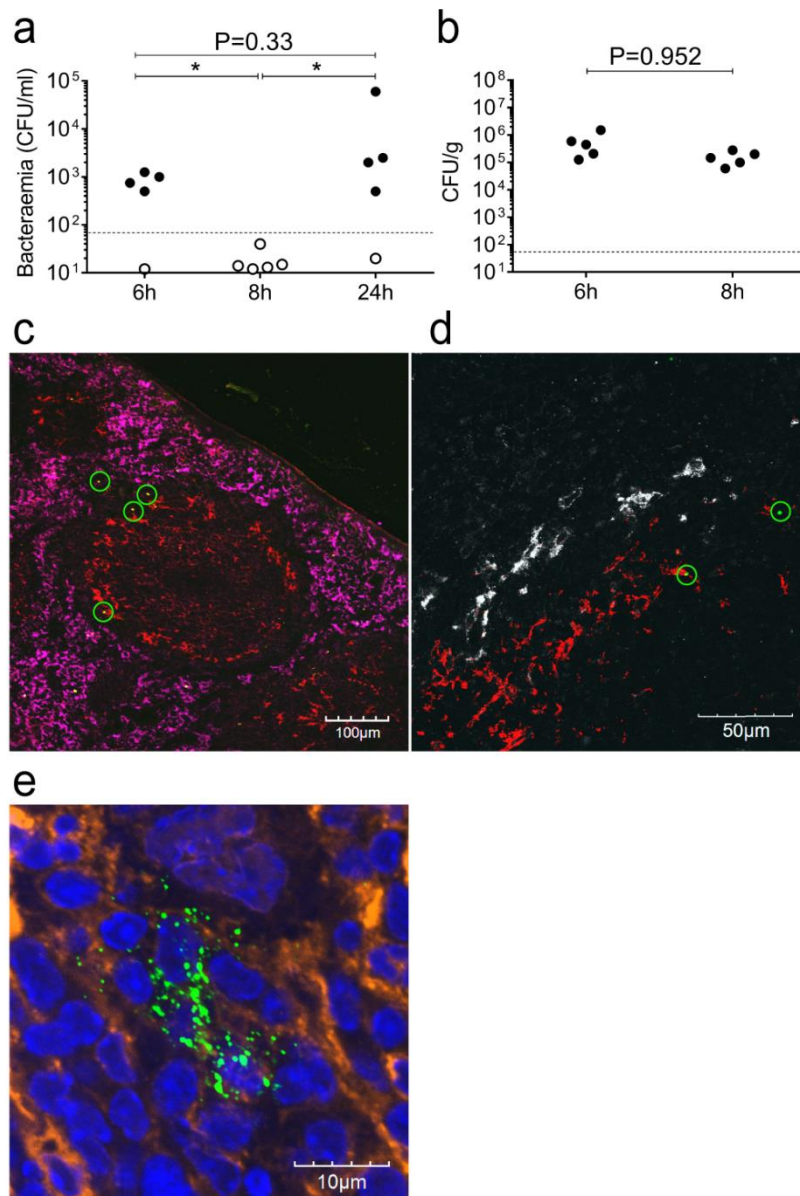
792 61 Taylor, P. R. *et al.* Development of a specific system for targeting protein to  
793 metallophilic macrophages. *Proceedings of the National Academy of Sciences of the*  
794 *United States of America* **101**, 1963-1968, doi:10.1073/pnas.0308490100 (2004).

795

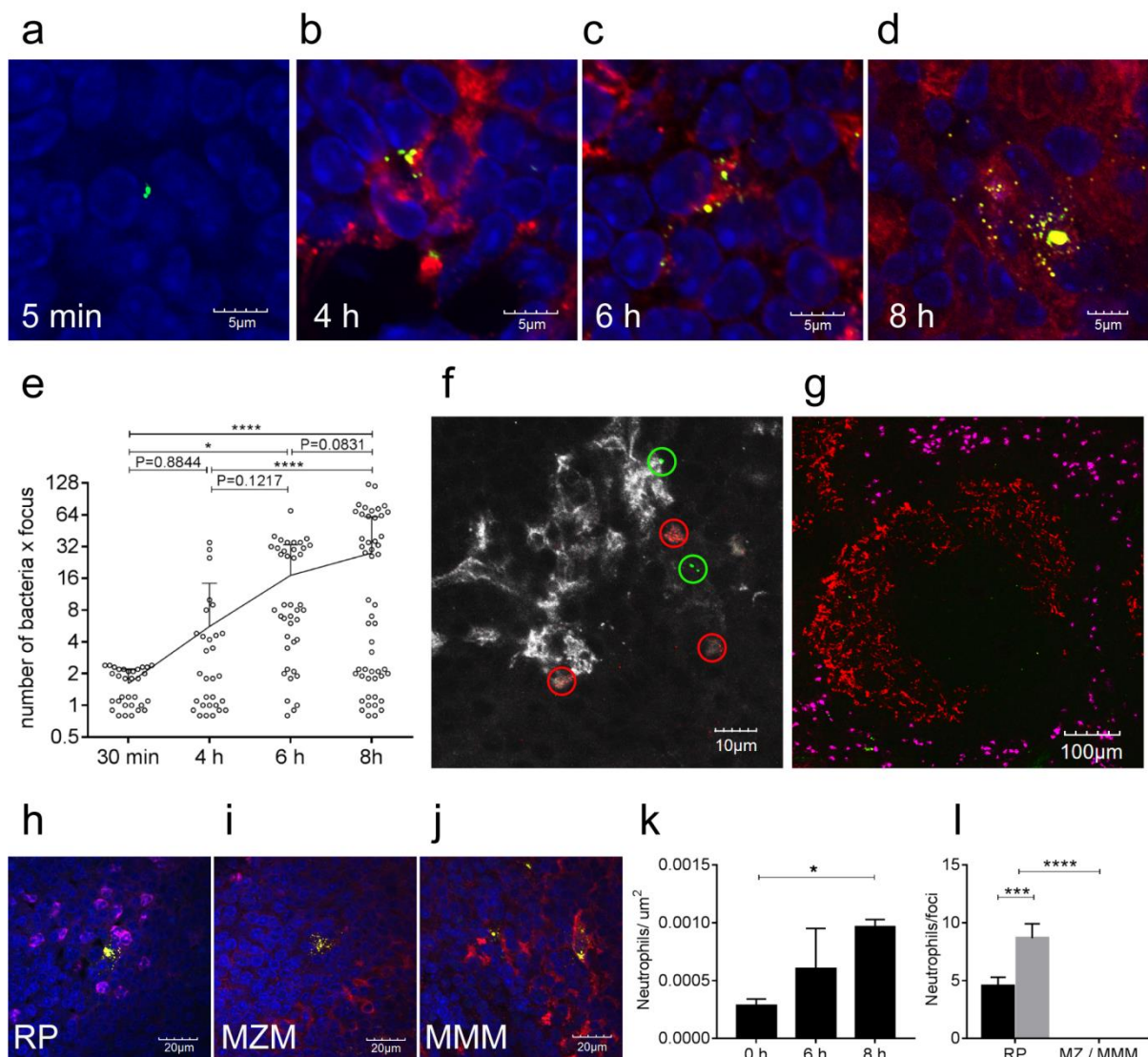
796

797

798



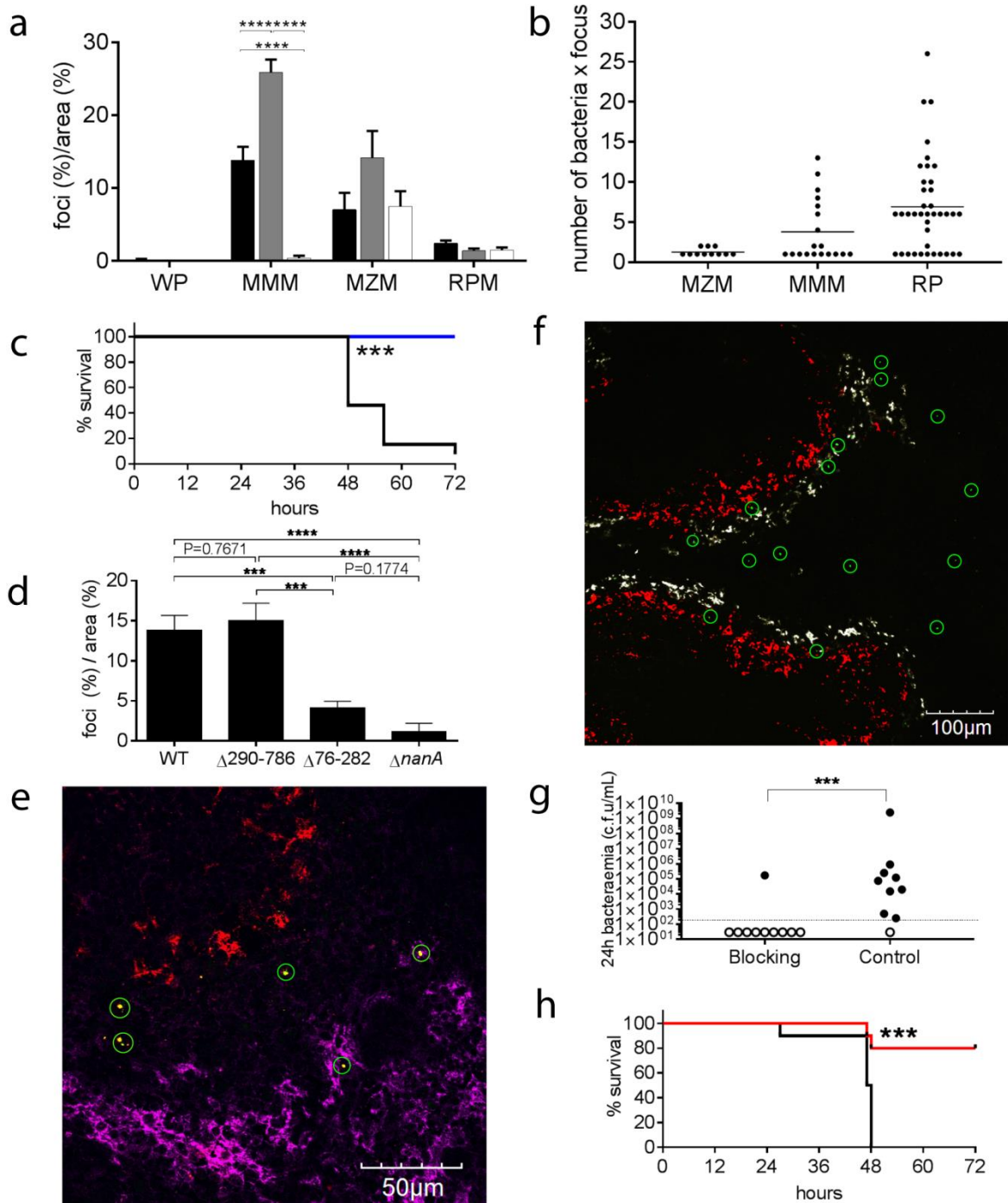
799  
800 **Figure 1: The eclipse phase of pneumococcal bacteraemia.** CD1 mice (n=15) were  
801 infected intravenously with  $1 \times 10^6$  pneumococci (strain D39). (a) Shows the numbers of  
802 bacteria in the blood at 6h, 8h and 24h (filled circles, positive blood cultures; empty circles,  
803 negative blood cultures). In the spleen (b), bacteria can be found both at 6h and at 8 h after  
804 inoculation. Values are expressed as CFU/ml in blood or CFU/g of spleen [weight 100 to 200  
805 mg]. The limit of detection is shown as a dotted line. Statistical differences (\*  $P < 0.05$ ,  
806 Fisher's exact test, one tailed) are indicated by thin black lines. Panels c to e show  
807 representative immunofluorescence microscopy images of on infected spleen sections.  
808 Single optical sections (analysis of 5 sections from 3 different spleens for each staining  
809 combination) obtained from 6 h infected spleens show the presence of bacterial clusters as  
810 small green dots (c, 20x objective and d, 60x objective) which can be seen as clusters of  
811 single bacteria at a higher magnification (e, 60x objective). In panel c bacteria are shown in  
812 green ( $\alpha$ -type2, AF488), bacterial foci are indicated by green circles, metallophilic  
813 macrophages in red (Cr-Fc, AF568b) and red pulp macrophages in magenta ( $\alpha$ -F4/80,  
814 AF647). In panel d, bacterial clusters (green circles,  $\alpha$ -type2, AF568) can be observed in the  
815 metallophilic macrophages area (Cr-Fc, AF647), in white marginal zone macrophages are  
816 also stained (aSIGN-R1b, AF488s). In panel e a big cluster of bacteria is shown in green ( $\alpha$ -  
817 type2, AF488), nuclei in blue (DAPI) and actin in orange (pAF647 conjugated phalloidin).  
818 Antibody details in Supplementary Table 1.



819  
820 **Figure 2: Numbers of pneumococci within clusters, founded by single cells, increase**  
821 **over time in the infected spleens.** (a-d) Immunofluorescence microscopy (representative  
822 of 5 sections from 3 different samples) on spleen sections of CD1 mice infected by *S.*  
823 *pneumoniae* D39 shows an increase of the number of bacteria in the foci of infection over  
824 time: (a) 5m; (b) 4h; (c) 6h and (d) 8 h. Splenic architecture was identified by staining the red  
825 pulp magenta ( $\alpha$ -F4/80, AF647), the metallophilic ring areas in red (Cr-Fc, AF568b) and  
826 nuclei in blue (DAPI). Bacteria (green,  $\alpha$ -type2, AF488) are trapped in the marginal sinus  
827 already at 30 minutes (a) and after an initial clearance, the number and size of the foci  
828 increased (b-c-d). A deeper analysis of those images further confirmed the increase of  
829 bacteria in time (e); for each time point, 25 microscope fields (60X magnification) were  
830 analysed to count the number of bacteria per focus (open circles) and number of foci. The  
831 trend line represents the arithmetic mean number of bacteria per focus, error bars show SD,  
832 statistical significance was determined using an ordinary one-way ANOVA with multiple  
833 comparisons. \*  $P < 0.05$ , \*\*\*\*  $p < 0.0001$ . A representative spleen section of mice infected with  
834 GFP-D39 and RFP-D39 ( $n=4$ ) labelled bacteria show how the pneumococci are present in  
835 clusters each of which is comprises either exclusively green or exclusively red fluorescent  
836 bacteria (green or red circles). Bacterial counts are shown in Supplementary Table 2. I In  
837 white metallophilic macrophages are also shown (Cr-Fc, AF568b) (f). In a representative  
838 spleen section 8 h after infection the neutrophil granulocytes in magenta ( $\alpha$ -GR1, AF647) are  
839 seen in the red pulp (g) and do not colocalise with marginal zone macrophages (Cr-Fc,  
840 AF568b). At a higher magnification (60x, panels h-j), the neutrophils were found to localise  
841 next to all foci of infection in the red pulp (RP,  $\alpha$ -F4/80, AF647) (h), but not in the marginal



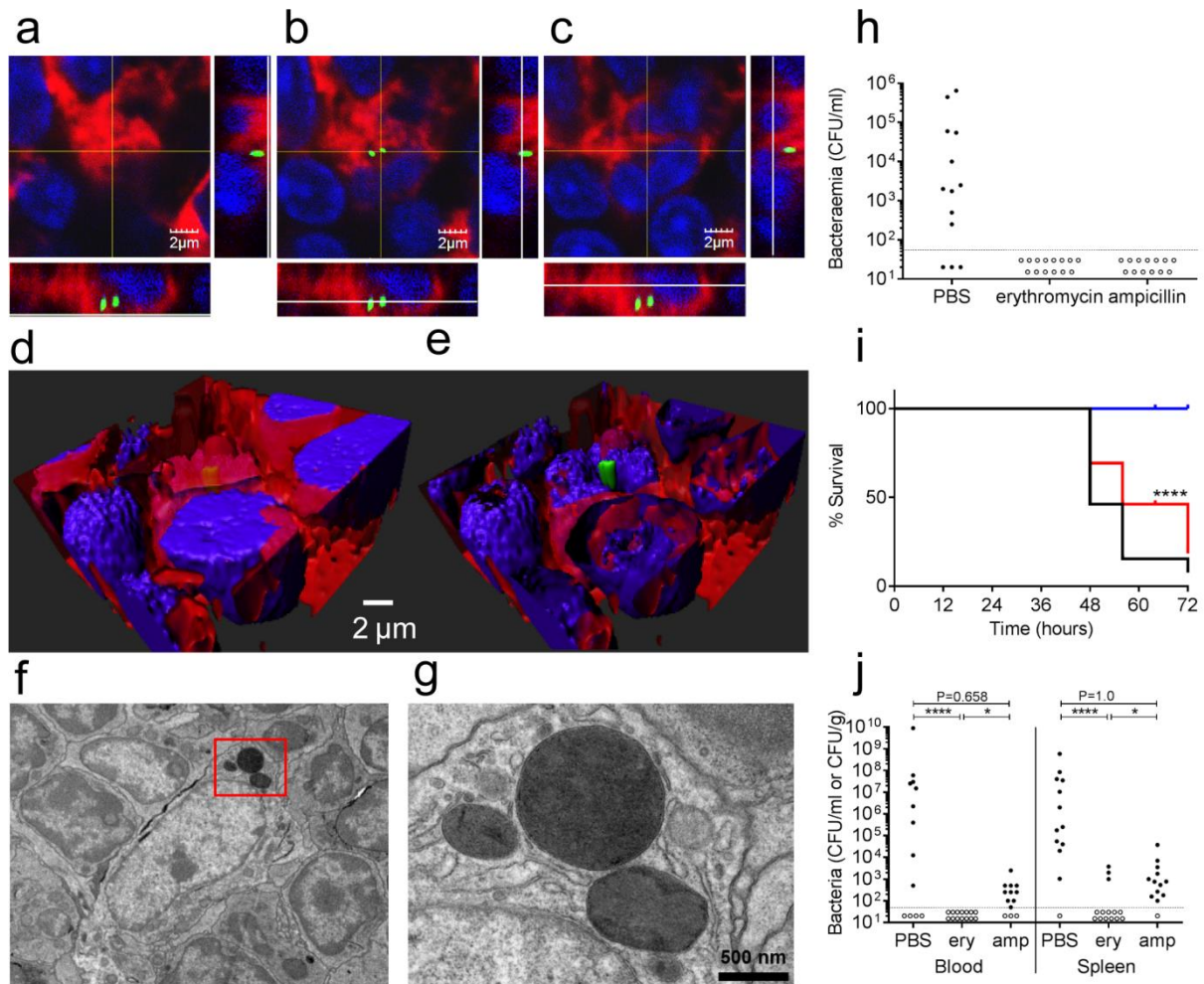
842 zone (MZM, nearby metallophilic macrophages are stained red, Cr-Fc, AF568b) (i) and in the  
843 metallophilic area (MMM, red, Cr-Fc, AF568b) (j). Five spleen sections from three mice each  
844 were analysed for this study, allowing for quantification of the number of neutrophils per  
845 square  $\mu\text{m}$  within the red pulp (k) and to quantify the number of neutrophils within a 25  $\mu\text{m}$   
846 radius of 5 or more discrete infectious foci in each zone of the spleen (l) (black bar 6h; grey  
847 bar 8 h). Error bars show SD, statistical significance was determined using a two tailed one-  
848 way ANOVA with Tukey's post correction, \*  $p < 0.05$ , \*\*\*  $P < 0.001$ , \*\*\*\*  $p < 0.0001$ . Antibody  
849 details are in Supplementary Table 1.  
850



851  
852  
853  
854  
855  
856  
857  
858  
859  
860  
861  
862  
863  
864

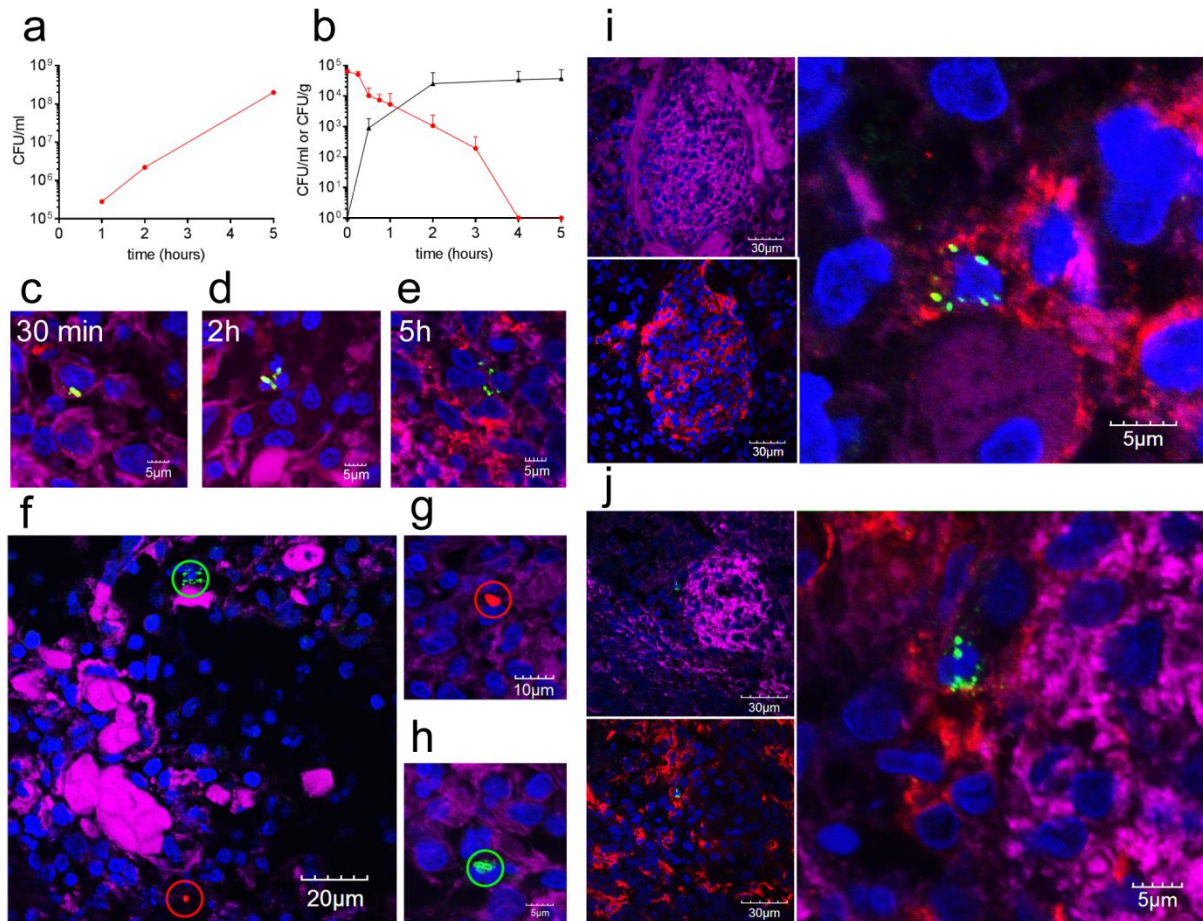
**Figure 3: Tissue localisation of infectious foci in the spleen.** Panel a shows the distribution of the foci of pneumococci at 6 h after infection normalized for the area of each spleen compartment (Supplementary Figure 4). Compartment analysed were the white pulp (WP), the metallophilic macrophage area (MMM), the marginal zone macrophage area (MZM) and the red pulp area (RP) of the spleen. Three infected mice groups have been considered for this analysis: mice infected with high dose ( $1 \times 10^6$  CFU) of *S. pneumoniae* (black bars), mice infected with low dose ( $1 \times 10^5$  CFU) (grey bars) and mice infected with  $1 \times 10^6$  CFU of the D39 after blocking with CD169 mAb (white bars). Counts were obtained from 30 random microscope fields from three independent infected spleens. Error bars show SD, Statistical differences in the percentages between the different infected groups are reported \*\*\*\*  $P < 0.0001$  (two-tailed one-way ANOVA). Number of bacteria per focus for the each spleen compartment are shown in panel b. Mean (lines) and SD (error bars) are reported. Panels c to e report data on mouse infections with the *nanA* mutants ( $n=22$ ).

865 Panel c shows the survival graph (black wt n=5, blue  $\Delta nanA$  n=5, \*\*\* P<0.001, kaplan-meier  
866 two-tailed test) and panel d the distribution of foci of infection in the metallophilic  
867 macrophages in mice infected with bacteria expressing wt NanA, no NanA ( $\Delta nanA$ ),  
868 NanA $\Delta$ 290-786 (sialidase domain deletion), and NanA $\Delta$ 76-282 (lectin domain deletion).  
869 Three independent spleens from mice infected with each *nanA* mutant were analysed to  
870 determine the localisation of foci. 20 fields were analysed from each spleen with a 40x  
871 objective. The data show the mean and standard deviation of 3 biological replicas. Statistical  
872 significance were determined using an ordinary one-way ANOVA with multiple comparisons,  
873 \*\*\* p<0.001, \*\*\*\* p<0.0001. Spleen section of D39 $\Delta nanA$  infected mice (panel e,  
874 representative of 5 sections from 3 different samples) show bacterial foci (green circles)  
875 localising exclusively to the marginal zone (not stained) or the red pulp. Red pulp  
876 macrophages are shown in magenta ( $\alpha$ -F4/80, AF647), metallophilic macrophages in red  
877 (Cr-Fc, AF568b) and bacteria in green ( $\alpha$ -type2, AF488). Panels from f to h show the data  
878 about blocking the CD169 receptor on metallophilic macrophages with a specific mAb (Rat  
879 IgG2a,k, Clone: 3D6.112) prior to infection. Panel f shows that in a representative spleen  
880 section (5 sections from 3 different samples), 4 hours after infection, bacterial clusters (green  
881 circles) do not localise anymore to the metallophilic macrophages (red) while they still are  
882 present in the marginal zone (white) or in the red pulp (black). Antibody details in  
883 Supplementary Table 1. Panel g shows the levels of bacteraemia 24 hours post-infection  
884 indicated by the number of CFU/mL of blood in mice treated with either anti-CD169 blocking  
885 antibody or with the isotype matched control (left, Isotype control, n=10, right, CD169 mAb,  
886 n=10). The dotted line indicates the limit of detection. Statistical significance were tested  
887 using a Mann-Whitney test. \*\*\* p<0.001. In panel h the survival graph of the same  
888 experiment is reported (black, Isotype control, n=10, red, CD169 mAb, n=10, \*\*\* P<0.001,  
889 kaplan-meier two-tailed test) .  
890



891  
 892  
 893  
 894  
 895  
 896  
 897  
 898  
 899  
 900  
 901  
 902  
 903  
 904  
 905  
 906  
 907  
 908  
 909  
 910  
 911  
 912  
 913  
 914  
 915  
 916

**Figure 4: The intracellular phase of *S. pneumoniae* in the early stages before overt septicaemia.** Panel a-c show three orthogonal views of intracellular pneumococci (green gfp), in this representative (5 sections from 3 different samples) multi-stack acquisition the green GFP-tagged bacteria are localised within the cytoplasm of the host cells 4 hours after the infection (60X magnification). The plasma membrane is shown in red (WGA 633 conjugated) and nuclei are stained in blue (DAPI). Three-dimensional reconstruction through deconvolution analysis clarifies the localisation of the pneumococci within the host cell (d-e). Further analysis with transmission electron microscopy identified groups of pneumococci in the cytoplasm of splenic macrophages. A representative image at 6000X magnification is shown in panel f (3 spleens analysed), while panel g is showing an enlarged insert of the same image (20000X magnification). The importance of the pneumococcal intracellular phase was assessed by treating CD1 mice after the infection (dose of  $1 \times 10^6$  CFU of strain D39) with antibiotics that have different penetration rates into the host cells (h-j). Two doses of both erythromycin (high penetration rate) and ampicillin (low penetration rate) were administered intraperitoneally at 1 and 5 h post-infection to groups of mice (12-13 animal per group). The doses were chosen so that the predicted drug half-life would reduce the drug plasma levels in 11 h to the minimal inhibitory concentration (MIC). Blood counts at 24 h after infection (panel h) show antibiotics to be equally effective in preventing bacteraemia in comparison to control ( $p < 0.001$ ). The limit of detection is shown as a dotted line. Analysis of later time points indicate that survival is greater significantly higher in the erythromycin group (blue) both with respect to the ampicillin group (red) and control (panel i). \*\*\*\*  $P < 0.0001$  kaplan-meier two-tailed test. Survival correlates to the terminal bacterial blood and spleen counts which are lower in erythromycin (ery) treated mice with respect to control in blood and to both control and ampicillin (amp) in the spleen (panel j). (\*\*\*\*  $P < 0.0001$ , \*  $P < 0.05$ , Fisher's exact test, one tailed)



917  
918  
919  
920  
921  
922  
923  
924  
925  
926  
927  
928  
929  
930  
931  
932  
933  
934  
935  
936  
937  
938  
939  
940  
941  
942

**Figure 5: The pig spleen perfusion as a model of infection with *S. pneumoniae*.** Pneumococci grow *in vitro* with a doubling time of approximately 45 min in heparinised porcine blood (a). In the *ex vivo* spleen perfusion model D39 pneumococci injected into the arterial circuit are taken up by the spleen and cleared from the blood over time (b). The data show the average number of CFU recovered from blood samples (red) and spleen biopsies (black) of three independent experiments. Error bars represent standard deviation. Immunofluorescence microscopy of infected spleen sections showed an increase of the size of the foci of infection over time (c-e). Bacteria were stained in green ( $\alpha$ -type2, AF488), CD169+ macrophages in red ( $\alpha$ -CD169p, AF568c) and nuclei in blue (DAPI). Actin staining (in magenta) was used to identify the endothelial tissue of the arterioles (pAF647 conjugated phalloidin). In five-hour infected spleen sections GFP-D39 (green) and RFP-D39 (red) labelled bacteria are present in foci of infection (circles) containing either exclusively green or exclusively red fluorescent bacteria respectively (f-h) (actin in magenta and nuclei in blue). Sections of five hours infected porcine spleens are shown in panels i and j. Clusters of pneumococci were found localised in the CD169+ macrophages of porcine spleens in the perifollicular sheath (i-j). Inserts to the left in both panel i and j show the microarchitecture evidenced by actin staining (magenta) and the distribution of CD169+ macrophages ( $\alpha$ -CD169p, AF568c), while the enlarged view is an enlarged view of the focus detected in the left upper panels. Staining was done as for Fig 5c. All the immunofluorescence images are representative of 5 sections from 3 different samples. Antibody details are in Supplementary Table 1.